Alcohol and Alcoholism, 2017, 52(3) 289–297
doi: 10.1093/alcalc/agx006
Advance Access Publication Date: 25 February 2017
Article

OXFORD

Article

Alcohol Induces Cellular Senescence and Impairs Osteogenic Potential in Bone Marrow-Derived Mesenchymal Stem Cells

Xi Chen[1,2,3,†], Mao Li[1,2,†], Jinku Yan[1,2], Tao Liu[1], Guoqing Pan[1,2], Huilin Yang[1,2], Ming Pei[4], and Fan He[1,2,*]

[1]Department of Orthopaedics, The First Affiliated Hospital of Soochow University, No. 188 Shizi Street, Suzhou 215153, Jiangsu, China, [2]Orthopaedic Institute, Medical College, Soochow University, No. 708 Renmin Road, Suzhou 215007, China, [3]School of Biology and Basic Medical Sciences, Medical College, Soochow University, No. 199 Renai Road, Suzhou 215123, China, and [4]Stem Cell and Tissue Engineering Laboratory, Department of Orthopaedics and Division of Exercise Physiology, West Virginia University, PO Box 9196, One Medical Center Drive, Morgantown, WV 26505-9196, USA

*Corresponding Author: Orthopaedic Institute, Soochow University, No. 708 Renmin Road, Suzhou 215007, Jiangsu, China. Tel: +86-512-67781420; Fax: +86-512-67781165; E-mail: fanhe@suda.edu.cn

[†]These authors are contributed equally to this work.

Received 2 November 2016; Accepted 9 January 2017

Abstract

Aims: Chronic and excessive alcohol consumption is a high-risk factor for osteoporosis. Bone marrow-derived mesenchymal stem cells (BM-MSCs) play an important role in bone formation; however, they are vulnerable to ethanol (EtOH). The purpose of this research was to investigate whether EtOH could induce premature senescence in BM-MSCs and subsequently impair their osteogenic potential.

Methods: Human BM-MSCs were exposed to EtOH ranging from 10 to 250 mM. Senescence-associated β-galactosidase (SA-β-gal) activity, cell cycle distribution, cell proliferation and reactive oxygen species (ROS) were evaluated. Mineralization and osteoblast-specific gene expression were evaluated during osteogenesis in EtOH-treated BM-MSCs. To investigate the role of silent information regulator Type 1 (SIRT1) in EtOH-induced senescence, resveratrol (ResV) was used to activate SIRT1 in EtOH-treated BM-MSCs.

Results: EtOH treatments resulted in senescence-associated phenotypes in BM-MSCs, such as decreased cell proliferation, increased SA-β-gal activity and G0/G1 cell cycle arrest. EtOH also increased the intracellular ROS and the expression of senescence-related genes, such as $p16^{INK4\alpha}$ and p21. The down-regulated levels of SIRT1 accompanied with suppressed osteogenic differentiation were confirmed in EtOH-treated BM-MSCs. Activation of SIRT1 by ResV partially counteracted the effects of EtOH by decreasing senescence markers and rescuing the inhibited osteogenesis.

Conclusion: EtOH treatments induced premature senescence in BM-MSCs in a dose-dependent manner that was responsible for EtOH-impaired osteogenic differentiation. Activation of SIRT1 was effective in ameliorating EtOH-induced senescence phenotypes in BMSCs and could potentially lead to a new strategy for clinically preventing or treating alcohol-induced osteoporosis.

Short summary: Ethanol (EtOH) treatments induce premature senescence in marrow-derived mesenchymal stem cells in a dose-dependent manner that is responsible for EtOH-impaired osteogenic differentiation. Activation of SIRT1 is effective in ameliorating EtOH-induced senescence phenotypes, which potentially leads to a new strategy for clinically treating alcohol-induced osteoporosis.

INTRODUCTION

Osteoporosis is a bone disorder characterized by reduced bone mass with increased susceptibility to fragility fractures. Osteoporotic fractures are strongly associated with increased morbidity and mortality, resulting in a drop in quality of patients' lives and an increase in medical costs. Common causes contributing to the development of osteoporosis include aging, low estrogen levels in postmenopausal women, long-term use of glucocorticoids and insulin-dependent diabetes mellitus (Rachner *et al.*, 2011). Among them, chronic and excessive alcohol consumption is recognized as a major cause of secondary osteoporosis in elderly men (Walsh and Eastell, 2013). Chronic heavy alcohol consumption, such as 100–200 g of alcohol per day, is considered a high-risk factor for loss of bone mineral density, impairment of bone remodeling and subsequent deterioration of bone tissue (Maurel *et al.*, 2012).

Bone remodeling mainly involves two stages: bone resorption and bone formation. Osteoblasts are essential for bone formation because of their capacity to synthesize collagenous and non-collagenous extracellular matrices and to promote matrix mineralization. Bone marrow-derived mesenchymal stem cells (BM-MSCs), as the major source of osteoblasts, were first identified through attachment onto plastic culture plates and characterized by their extensive self-renewal capacity and multi-lineage differentiation potentials (Pittenger *et al.*, 1999). A growing amount of evidence has demonstrated that the lineage-specific differentiation of BM-MSCs, such as osteogenesis and adipogenesis, plays an important role in the pathology of osteoporosis, as evidenced by the fact that the shift of BM-MSC differentiation into an adipocyte lineage results in excessive fat production and inadequate bone formation (Nuttall and Gimble, 2000; Chen *et al.*, 2015). A recent study confirmed that MSCs isolated from ovariectomized rats showed lower osteogenic potential in contrast to relatively higher adipogenic potential as compared with normal rats (Pei *et al.*, 2015).

Similar to other somatic cells, BM-MSCs have a limited replicative capacity and eventually undergo a process of cellular senescence. In particular, oxidative stress environments at pathological or injured tissue sites, such as osteoarthritis or bone fracture, result in DNA damage in recruited BM-MSCs and the failure to repair DNA damage leads to premature senescence in BM-MSCs (Li and Pei, 2012). Senescent cells are characterized by enlarged cell shape, irreversible cell cycle arrest, loss of cell proliferation and increased senescence-associated β-galactosidase (SA-β-gal) activity (Vidal *et al.*, 2012). Moreover, senescent BM-MSCs exhibit impaired multi-lineage differentiation potentials that not only decelerate the rate of bone formation but also increase the propensity for osteoporosis (Aldahmash, 2015). Bonyadi *et al.* showed that inhibition of BM-MSC self-renewal resulted in loss of bone mass and subsequent age-dependent osteoporosis (Bonyadi *et al.*, 2003). Recently, human silent information regulator Type 1 (SIRT1), a member of the nicotinamide adenine dinucleotide-dependent deacetylase protein family, has been proposed to be a critical modulator of cell functions such as energy metabolism, inflammation, stress resistance, cellular senescence and survival/death decision (Fusco *et al.*, 2012; Zhou *et al.*, 2015). SIRT1 mediates its physiological functions mainly by deacetylating histones, transcription factors or coactivators. For example, in response to oxidative stress-induced DNA damage, SIRT1 binds and deacetylates p53, a cell cycle regulator, thus suppressing transcription of its down-stream genes such as p21 (Vaziri *et al.*, 2001). A recent study demonstrated that cord blood endothelial progenitor cells isolated from premature neonates displayed an accelerated senescence due to the decrease in SIRT1 and the increase in $p16^{INK4\alpha}$, whereas an overexpression of SIRT1 reversed senescent phenotypes and restored the capacity for neovessel formation (Vassallo *et al.*, 2014). SIRT1 has also been proven to control the lineage commitment of BM-MSCs toward osteoblasts, in a means other than adipocytes, by up-regulating expression of osteo-lineage genes (Tseng *et al.*, 2011).

Previous studies have shown the inhibitory effects of alcohol on osteogenic differentiation of BM-MSCs, as evidenced by decreased levels of collagen synthesis and matrix mineralization (Gong and Wezeman, 2004). However, little is known about whether or not alcohol exposure could induce premature senescence in BM-MSCs and the underlying molecular mechanisms are unclear. In this study, we hypothesized that exposure of BM-MSCs to alcohol-induced premature senescence and subsequently suppressed their osteogenic potential via deactivating SIRT1. We tested the effects of alcohol ranging from 10 to 250 mM on induction of premature senescence-associated phenotypes in BM-MSCs. The dose of 50 mM has been suggested to be modest but effective in suppressing cell proliferation (Gong and Wezeman, 2004). Furthermore, the concentration of alcohol at 10 and 250 mM was chosen to mimic slight and heavy alcohol consumption, respectively. To illustrate the role of SIRT1 in EtOH-induced premature senescence, resveratrol (ResV), a SIRT1 activator, was used to counteract EtOH effects and underlying mechanisms involving the SIRT1 signaling pathway were investigated.

MATERIALS AND METHODS

Reagents

Human BM-MSCs (Cat. HUXMA-01001) were purchased from Cyagen Biosciences Inc. (Guangzhou, China). Fetal bovine serum (FBS; Cat. 16000044), alpha minimum essential medium (α-MEM; Cat. 12571063), Dulbecco's modified Eagle medium (DMEM; Cat. 10567014) and protease inhibitor tablets (Cat. 88665) were purchased from Thermo Fisher Scientific (Waltham, MA, USA). Penicillin–Streptomycin (Cat. 15140122), 4′,6-diamidino-2-phenylindole (DAPI; Cat. 62247) and TRIzol® reagent (Cat. 15596018) were purchased from Invitrogen (Carlsbad, CA, USA). EtOH (Cat. E7023), ResV (Cat. R5010), propidium iodide (PI; Cat. 81845), RNase A (Cat. R6513), dexamethasone (Cat. D4902), L-ascorbic acid (Cat. 95437), β-glycerol phosphate (Cat. 50020) and fluorescein diacetate (FDA; Cat. F7378) were obtained from Sigma-Aldrich (St. Louis, MO, USA). Primary antibodies against $p16^{INK4\alpha}$ (Cat. ab51243), SIRT1 (Cat. ab110304), p38 (Cat. ab31828), p-p38 (phospho T180 + Y182; Cat. ab4822), p21 (Cat. ab109199), glyceraldehyde-3-phosphate dehydrogenase (GAPDH; Cat. ab8245) and horseradish peroxidase-conjugated secondary antibodies (Cat. ab6728) were purchased from Abcam (Cambridge, MA, USA). This project was approved by the Ethics Committee of the First Affiliated Hospital of Soochow University (No. 2015-059).

Cell culture

BM-MSCs were initially seeded in tissue culture polystyrene plates at the density of 5000 cells/cm^2 in growth medium (α-MEM supplemented with 10% FBS, 100 U/ml of penicillin and 100 μg/ml of streptomycin) at 37°C in a 5% CO_2 incubator. To examine whether EtOH would induce premature senescence in BM-MSCs, cells were exposed to 10, 50 and 250 mM EtOH (diluted in growth medium) for 7 days; untreated cells served as the control group. For the experiment investigating the role of SIRT1 in EtOH-mediated senescence, BM-MSCs were treated with 10 μM ResV (a SIRT1 agonist) in the presence of 250 mM EtOH.

Cell viability assay

Cells were washed with phosphate buffered saline and incubated in 5 μg/ml of FDA solution at 37°C for 10 min. The fluorescence images were captured at a ×100 magnification using an Olympus IX51 microscope (Olympus Corporation, Tokyo, Japan).

Cell proliferation assay

Cell proliferation was evaluated using a cell counting kit-8 (CCK-8; Cat. C0037; Beyotime Institute of Biotechnology, Haimen, China). Using 96-well plates, 10 μl of CCK-8 solution was added to each well and the cells were incubated at 37°C for 1 h. Absorbance was determined at 450 nm using a microplate spectrophotometer (BioTek, Winooski, VT, USA). The absorbance values were normalized to the level of the control group.

Cell cycle analysis

After treating with EtOH, BM-MSCs were dissociated and fixed in 70% ethanol (EtOH) at 4°C for 24 h. Cells were stained with 50 μg/ml PI and 50 μg/ml RNase A at 37°C for 30 min. Samples were analyzed using a Cytomics FC500 Flow Cytometer (Beckman Coulter, Brea, CA, USA) and at least 5000 cells were collected per sample. The data were analyzed using the MultiCycle AV DNA analysis software (Phoenix Flow Systems, San Diego, CA, USA).

SA-β-gal staining

The positive blue staining of SA-β-gal (pH = 6.0) is a typical biomarker of premature senescence. The SA-β-gal stain was performed using an SA-β-gal staining kit (Cat. C0602; Beyotime), according to the manufacturer's instructions. The cells were incubated overnight at 37°C without CO2 and nuclei were counterstained with DAPI. To quantify the percentage of SA-β-gal-positive cells, an Olympus IX51 microscope-captured digital images in 10 randomly chosen fields and a total of at least 200 cells from each sample were counted to calculate the percentage of senescent cells.

Intracellular ROS measurement

Intracellular levels of reactive oxygen species (ROS) were quantified through a fluorescent method. About 2×10^5 cells were incubated in 10 μM 2′,7′-dichlorofluorescein diacetate (Cat. 35845; Sigma) at 37°C for 10 min. The fluorescence intensity was measured using a Cytomics FC500 Flow Cytometer and 10,000 events from each cell sample were analyzed using the WinMDI (Windows Multiple Document Interface for Flow Cytometry) 2.9 software.

Osteogenic differentiation and alizarin red S staining

BM-MSCs were cultured in osteogenic differentiation medium (DMEM supplemented with 10% FBS, 100 U/ml penicillin, 100 μg/ml streptomycin, 50 μg/ml L-ascorbic acid, 100 nM dexamethasone and 10 mM β-glycerol phosphate) for 21 days. The differentiation medium was changed every 3 days. Mineralization of the matrix was determined by Alizarin Red S staining. Cells were fixed in 4% paraformaldehyde (Sigma-Aldrich) and incubated in 1% Alizarin Red S solution (pH = 4.3; Cat. A5533; Sigma-Aldrich) for 15 min. Images of calcium deposition were captured using an Olympus IX51 microscope. To quantify the calcified matrix, 200 μl of 5% perchloric acid (Cat. 244252; Sigma-Aldrich) was added to each well and absorbance was measured at 420 nm using a microplate spectrophotometer.

Total RNA extraction and real-time RT-PCR

Total RNA was extracted using TRIzol® reagent; 1 μg of total RNA was reverse-transcribed using the RevertAid First Strand cDNA Synthesis Kit (Cat. K1622; Thermo Fisher). To quantify mRNA expression, an amount of cDNA equivalent to 50 ng of total RNA was amplified by real-time PCR using the iTap™ Universal SYBR® Green Supermix kit (Cat. 1725125-c; Bio-Rad, Hercules, CA, USA). The primer sequences were as follows: 5′-CCCAACGCACCGAATAGT-3′ (forward) and 5′-ATCTAAGTTTCCCGAGGTT-3′ (reverse) for *P16INK4A*, 5′-GCGGGAATCCAAAGGATAAT-3′ (forward) and 5′-CTGTTGCAAAGGAACCATGA-3′ (reverse) for *SIRT1*, 5′-GCGGGAATCCAAAGGATAAT-3′ (forward) and 5′-CTGTTGCAAAGGAACCATGA-3′ (reverse) for *P21*, 5′-CAGCCGCTTCACCTACAGC-3′ (forward) and 5′-TTTTGTATTCAATCACTGTCTTGCC-3′ (reverse) for *COL1A1* (Type I collagen α1), 5′-AGAAGGCACAGACAGAAGCTTGA-3′ (forward) and 5′-AGGAATGCGCCCTAAATCACT-3′ (reverse) for *RUNX2* (runt-related transcription factor 2), 5′-GAGCCCCAGTCCCCTACC-3′ (forward) and 5′-GACACCCTAGACCGGGCCGT-3′ (reverse) for *BGLAP* (bone gamma carboxyglutamate protein or osteocalcin), and 5′-AGAAAAACCTGCCAAATATGATGAC-3′ (forward) and 5′-TGGGTGTCGCTGTTGAAGTC-3′ (reverse) for *GAPDH*. Real-time PCR was performed on a CFX96™ Real-Time PCR System (Bio-Rad) following the manufacturer's protocol. Relative transcript levels of senescence-associated and osteogenic genes were normalized with the GAPDH internal control and were calculated using the $2^{-\Delta\Delta Ct}$ method.

Western blot analysis

Cells were lysed in ice-cold cell lysis buffer (Cat. P0013; Beyotime) containing protease inhibitors and the protein concentration in the cell extracts was quantified using a bicinchoninic acid protein assay kit (Cat. P0010; Beyotime). Equal amounts of protein (40 μg) from each extract were denatured and separated in a 10% polyacrylamide gel (Cat. 0012 A; Beyotime), and then transferred by electrophoresis onto a nitrocellulose membrane (Cat. LC2001; Thermo Fisher). The membrane was incubated in properly diluted primary antibodies at 4°C overnight, and then incubated in secondary antibodies (Abcam) at room temperature for 1 h. The membranes were developed using SuperSignal West Pico Substrate (Cat. 34579; Thermo Fisher) and CL-XPosure Film (Cat. 34097; Thermo Fisher). The intensity of bands was quantified using ImageJ software (National Institutes of Health, Bethesda, MD, USA).

Statistical analysis

Statistical analysis was conducted using the SPSS 13.0 statistical software (SPSS Inc., Chicago, IL, USA). All data were expressed as means ± standard deviation (SD). Statistical differences were determined using the two-tailed Student's *t*-test and the analysis of variance with a Tukey's *post hoc* test for multiple group comparisons. Significance was indicated by a P-value < 0.05 (*).

RESULTS

EtOH suppresses cell proliferation and up-regulates CDKIs

To evaluate the effects of EtOH on cell morphology and proliferation, BM-MSCs were treated with EtOH at varied concentrations (10, 50 and 250 mM) for 7 days. FDA staining suggested that BM-MSCs lost their spindle-like morphology and became a flattened cell shape following EtOH treatment. EtOH-treated BM-MSCs also showed a decreased cell density compared to untreated cells (Fig. 1a).

The CCK-8 assay confirmed that EtOH treatment suppressed cell proliferation by 16.3% at 50 mM, and 41.7% at 250 mM, compared to the untreated group (Fig. 1b). The results of cell cycle phase distribution suggested that EtOH at 250 mM induced BM-MSCs into a G0/G1 cell cycle arrest (Fig. 1c). The proportion in the G0/G1 phase of the 250 mM group (79.7 ± 3.3%) was significantly higher than the other three groups and EtOH-treated cells showed a decreased proportion in the S phase (10.3 ± 1.5% at 0 mM, 8.9 ± 2.0% at 10 mM, 6.5 ± 1.9% at 50 mM and 3.9 ± 0.8% at 250 mM) (Fig. 1d). We further examined the mRNA and protein levels of two cyclin-dependent kinases inhibitors (CDKIs), $p16^{INK4\alpha}$ and p21. Both the treatment with 50 and 250 mM EtOH significantly increased the transcript levels of *P16INK4A* (Fig. 1e) and *P21* (Fig. 1f) by 67.5% and 40.4%, respectively. Western blot analysis confirmed that EtOH treatment up-regulated the protein levels of $p16^{INK4\alpha}$ and p21 (Fig. 1g).

EtOH induces premature senescence and inhibits SIRT1 in BM-MSCs

To evaluate the effect of EtOH on premature senescence of BM-MSCs, SA-β-gal staining was used to label the senescent cells (Fig. 2a). In untreated cells, only 13.1 ± 4.6% cells were positive for SA-β-gal staining but, after exposure to EtOH, the percentage of SA-β-gal-positive cells increased to 17.6 ± 6.4% at 10 mM, 36.2 ± 3.9% at 50 mM and 56.9 ± 6.8% at 250 mM (Fig. 2b). To investigate the underlying mechanisms by which EtOH-induced premature senescence, intracellular levels of ROS were analyzed (Fig. 2c). Flow cytometry data suggested that treatment with 250 mM EtOH significantly increased ROS by 82.2%, compared to that of untreated cells (Fig. 2d). To determine the roles of SIRT1 and p38 in EtOH-induced senescence, we measured the expression of SIRT1 and phosphorylated levels of p38. The mRNA levels of *SIRT1* in BM-MSCs decreased upon treatment with EtOH (Fig. 2e) and the protein levels were confirmed by western blot analysis. We found that exposure to EtOH enhanced phosphorylation of p38 in BM-MSCs in a dose-dependent manner; however, the total p38 protein expression was similar in all groups (Fig. 2f).

EtOH-induced senescence correlates with inhibited osteogenic differentiation of BM-MSCs

The osteogenic differentiation potential of BM-MSCs is crucial to the quality of bone formation; therefore, we analyzed whether the propensity for osteogenesis was suppressed by EtOH-induced premature senescence. Alizarin Red S staining was used to determine mineralized matrix production after a 21-day differentiation induction (Fig. 3a) and, in EtOH-treated cells, the level of matrix mineralization decreased by 35.2% at 50 mM and 91.7% at 250 mM compared to untreated cells (Fig. 3b). Real-time reverse transcription-polymerase chain

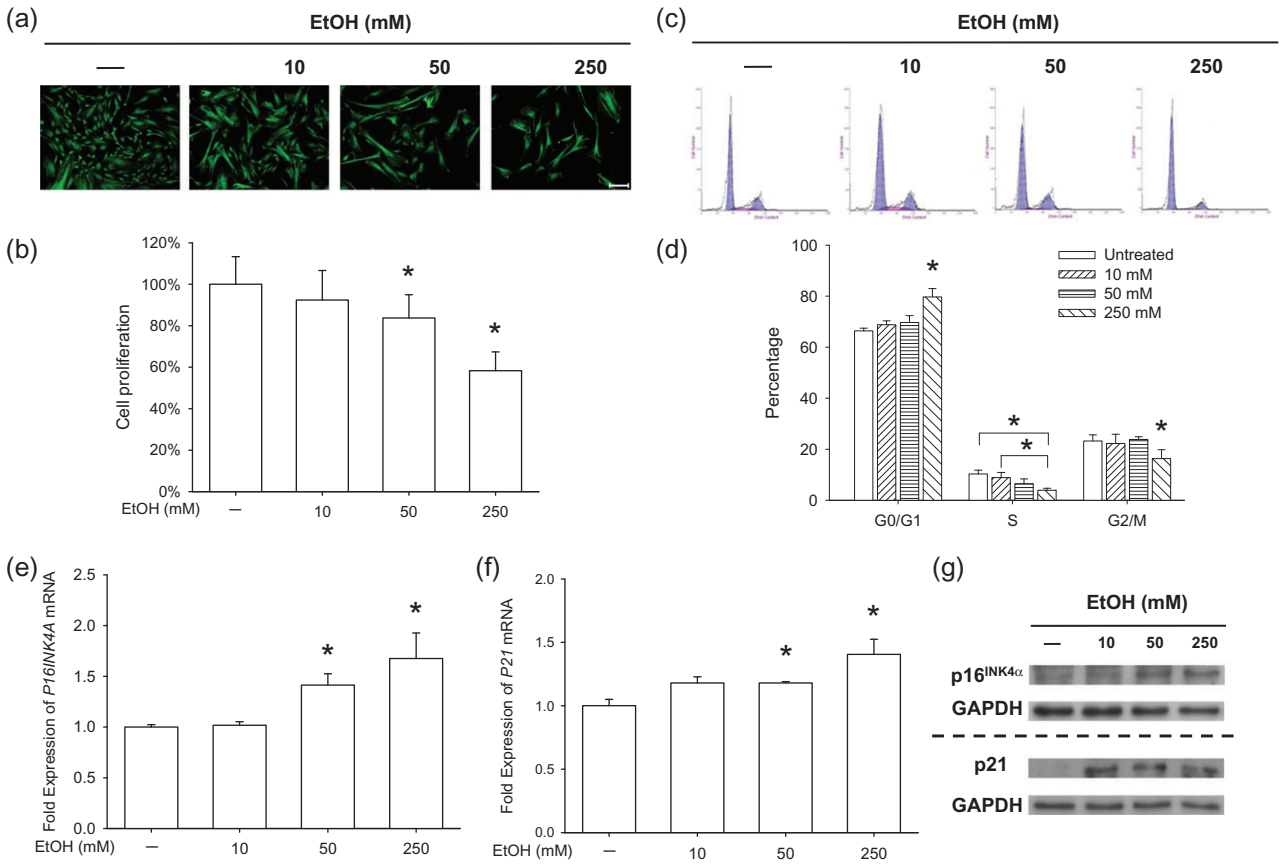

Fig. 1. The treatments with EtOH suppressed cell proliferation and up-regulated CDKIs. (**a**) Representative images labeled by FDA showed cell density and morphology of BM-MSCs. Scale bar = 200 μm. (**b**) Cell proliferation was determined by the CCK-8 assay. Absorbance was determined at 450 nm and was normalized to the level of untreated cells. (**c–d**) Flow cytometry analysis was used to measure the cell cycle distribution of EtOH-treated BM-MSCs. (**e–f**) The mRNA levels of *P16INK4A* (**e**) and *P21* (**f**) were measured by real-time RT-PCR. (**g**) Western blot was used to measure the protein levels of $p16^{INK4\alpha}$ and p21. Values are the mean ± SD of eight independent experiments ($n = 8$) in CCK-8 assays, three independent experiments ($n = 3$) in cell cycle analysis and four independent experiments ($n = 4$) in real-time RT-PCR experiments. Statistically significant differences are indicated by $^*P < 0.05$.

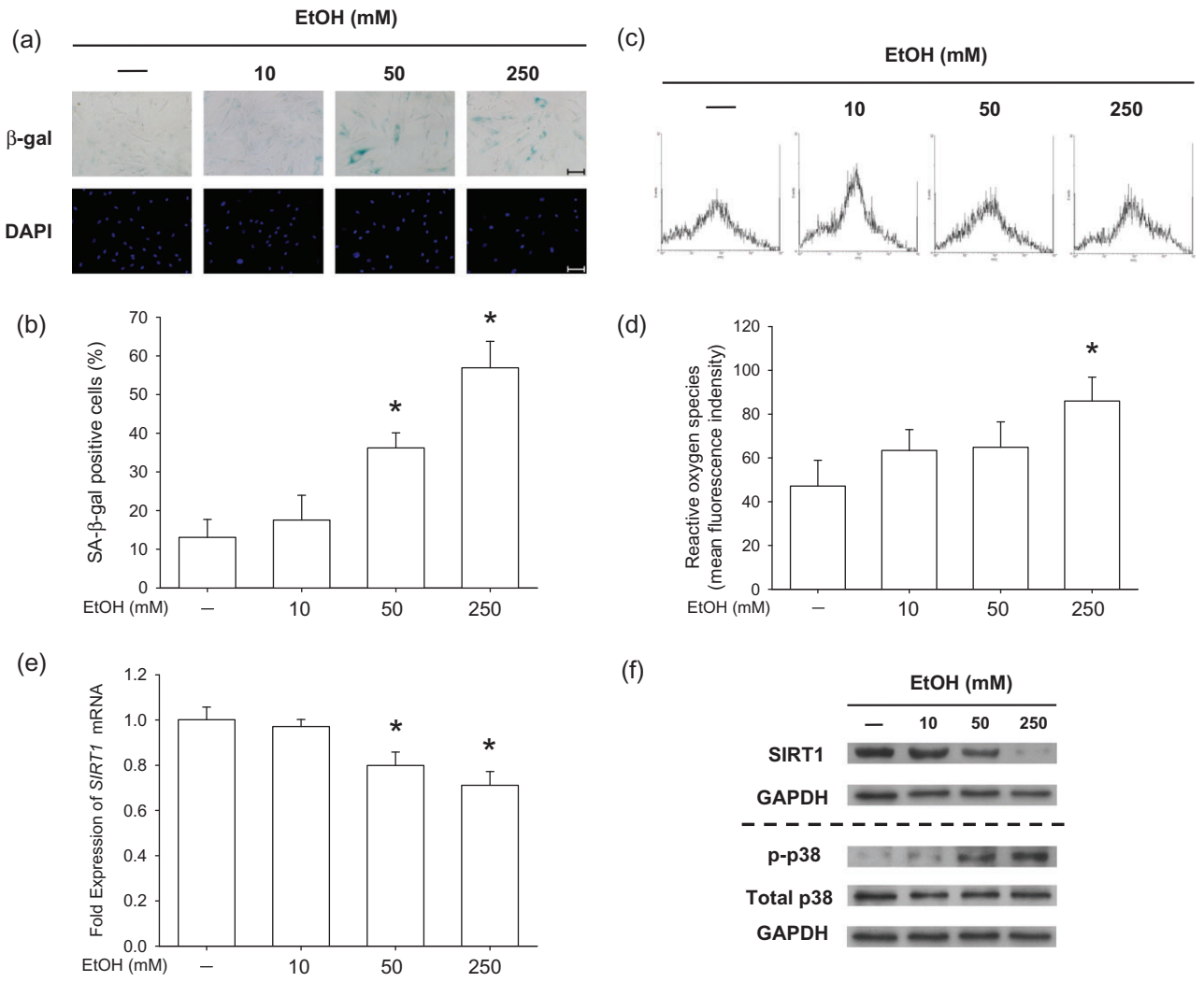

Fig. 2. The treatments with EtOH-induced premature senescence and inhibited SIRT1 in BM-MSCs. (**a**) Representative images of senescent cells that were stained for SA-β-gal and the nuclei were counterstained with DAPI. Scale bar = 100 μm. (**b**) Quantification of the percentage of SA-β-gal-positive cells that were induced by EtOH. (**c**) Representative data of intracellular ROS that were measured by flow cytometry. (**d**) Quantification of intracellular ROS in EtOH-treated BM-MSCs. (**e**) The mRNA levels of SIRT1 in EtOH-treated cells. (**f**) Protein levels of SIRT1 and phosphorylated levels of p38 were analyzed by western blot. Values are the mean ± SD of four independent experiments ($n = 4$) in ROS assays and real-time RT-PCR experiments. Statistically significant differences are indicated by $^*P < 0.05$.

reaction (RT-PCR) data showed that treatments with 50 and 250 mM EtOH down-regulated *COL1A1* transcription by 7.2% and by 38.7%, respectively, compared to the control group (Fig. 3c). The transcript levels of the *RUNX2* gene decreased in EtOH-treated cells in a dose-dependent manner, by 18.7% at 10 mM, 19.1% at 50 mM and 38.0% at 250 mM, compared to the control group (Fig. 3d). Similarly, treatments with 50 and 250 mM EtOH suppressed the mRNA levels of *BGLAP* by 12.1% and by 25.9%, respectively (Fig. 3e). These results suggest that osteogenic differentiation of BM-MSCs was inhibited by EtOH-induced premature senescence.

Activating SIRT1 by ResV protects BM-MSCs from EtOH-induced premature senescence

To confirm whether EtOH-induced premature senescence was mediated by inhibiting SIRT1 in BM-MSCs, we used 10 μM ResV (Tseng *et al.*, 2011) to specifically activate SIRT1 in the presence of 250 mM EtOH. FDA immunofluorescence staining showed that treatment with ResV increased cell density (Fig. 4a) and CCK-8 results confirmed that cell proliferation of the ResV + EtOH group increased by 31.1% compared to that of the EtOH group (Fig. 4b). Flow cytometry data showed that supplementation with ResV attenuated the level of intracellular ROS by 25.7% in BM-MSCs when exposed to EtOH (Fig. 4c). Real-time RT-PCR data showed that, in EtOH-treated cells, treatment with ResV decreased the gene expression of *P16INK4A* (Fig. 4d) and *P21* (Fig. 4e) by 19.9% and 23.2%, respectively. In contrast, ResV increased the transcript level of *SIRT1* in EtOH-treated cells by 25.8% (Fig. 4f). Western blot analysis confirmed that treatment with ResV reduced EtOH-induced up-regulation of $p16^{INK4\alpha}$ and p21 and increased the level of SIRT1 (Fig. 4 g). Furthermore, we found that the phosphorylated levels of p38 were attenuated by treatment with ResV.

ResV rescues EtOH-inhibited osteogenic differentiation

To further investigate the role of SIRT1 in EtOH-inhibited osteogenic differentiation, ResV (10 μM) was used to activate SIRT1

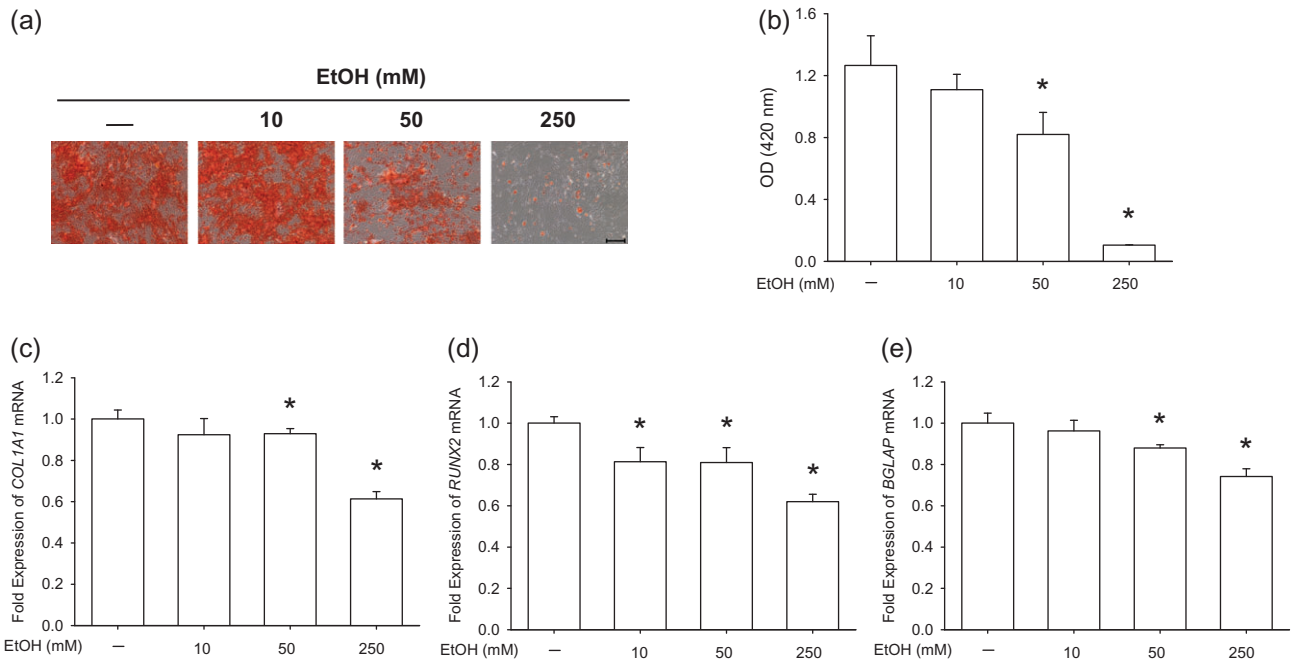

Fig. 3. EtOH impaired the osteogenic potential of BM-MSCs. (**a**) Representative images of mineralized extracellular matrix stained by Alizarin Red S. Scale bar = 200 μm. (**b**) Quantification of matrix mineralization. The stained mineral layers were treated with perchloric acid and absorbance was measured at 420 nm. **(c–e)** The mRNA levels of osteoblast-specific marker genes, including *COL1A1* (**c**), *RUNX2* (**d**) and *BGLAP* (**e**) were measured by real-time RT-PCR. Values are the mean ± SD of four independent experiments ($n = 4$) in Alizarin Red S staining and real-time RT-PCR experiments. Statistically significant differences are indicated by $^*P < 0.05$.

in EtOH-treated BM-MSCs (250 mM) during osteogenesis. Mineralization of the matrix demonstrated that supplementation of ResV increased the mineralization level by 3.4-fold compared to EtOH-treated cells, though the level was significantly lower than that of untreated cells (Fig. 5a and b). Transcript levels of osteoblast-specific genes also suggested that activation of SIRT1 by ResV partially restored osteogenic differentiation of BM-MSCs, which was inhibited by EtOH. Treatment with ResV significantly up-regulated the gene expression of *COL1A1* by 24.5% (Fig. 5c), *RUNX2* by 63.8% (Fig. 5d) and *BGLAP* by 22.6% (Fig. 5e), as compared to EtOH-treated cells.

DISCUSSION

The causes of cellular senescence in BM-MSCs include over-proliferation, telomere shortening and an oxidative stress environment. For oxidative stress-induced premature senescence, not only exogenous hydrogen peroxide (H_2O_2) at moderate concentrations (100–200 μM) (Ko *et al.*, 2012) but also over-accumulation of intracellular ROS, have been demonstrated to trigger the onset of senescence (Ho *et al.*, 2013), resulting in proliferative decline and differentiation alteration. In this study, we found that intracellular ROS of BM-MSCs increased after exposure to EtOH and, subsequently, senescence-associated phenotypes were observed, such as cell cycle arrest and increased SA-β-gal activity. Elevated levels of EtOH-induced ROS might be responsible for increased senescence markers in BM-MSCs. This result was consistent with a previous report in which intracellular β-gal activity was confirmed positive and senescence-associated transcriptional factors increased in EtOH-treated osteoblasts (Chen *et al.*, 2009). According to previous studies, the concentration of alcohol at 50 mM was effective in suppressing osteoblast differentiation *in vitro* (Gong and Wezeman, 2004) and to shift the lineage commitment of BM-MSCs toward adipocytes (Wezeman and Gong, 2004). In this study, the usage of a high EtOH dose for treatment was done to show distinct senescence-associated phenotypes and to allow a variety of concentrations to determine if the results responded in a dose-dependent manner. With a concentration of 250 mM EtOH, we tried to induce premature senescence in *in vitro*-cultured BM-MSCs within a short period in order to avoid replicative senescence. Further *in vivo* studies are necessary to prove that BM-MSCs from patients or animals with alcohol-induced osteopenia would tend to display senescence-associated phenotypes compared with untreated cells.

Accumulating data have shown that excessive production of ROS is responsible for oxidative DNA damage and consequent cellular senescence in stem cells (Yahata *et al.*, 2011). EtOH-induced oxidative stress resulted in DNA damage and defective DNA repair, possibly through inhibiting crucial DNA repair factors, such as 53BP1 (Romero *et al.*, 2016). The improperly repaired DNA damage further activated several cell cycle checkpoint proteins, such as p53 and $p16^{INK4\alpha}$, and led to the onset of premature senescence. In osteoblasts, a 48-h treatment with EtOH activated the cell cycle inhibitor p53 and its transcriptional target p21, both of which were responsible for the initiation of cellular senescence (Chen *et al.*, 2009). In this study, we found that treatments with EtOH significantly up-regulated the mRNA and protein levels of $p16^{INK4\alpha}$. The protein $p16^{INK4\alpha}$ is an important regulator in cell cycle by assisting transition from the G1 phase to the S phase and has been suggested as a hallmark of aged or senescent cells (Krishnamurthy *et al.*, 2004). Therefore, our results suggested that EtOH-induced premature senescence was mediated through increased levels of ROS and cell cycle regulators p21 and $p16^{INK4\alpha}$.

In the search for the underlying mechanisms by which EtOH-induced premature senescence in BM-MSCs, we found that p38 was activated in senescent cells after exposure to EtOH. The inhibition of p38 by SB203580 was sufficient to prevent senescence markers by

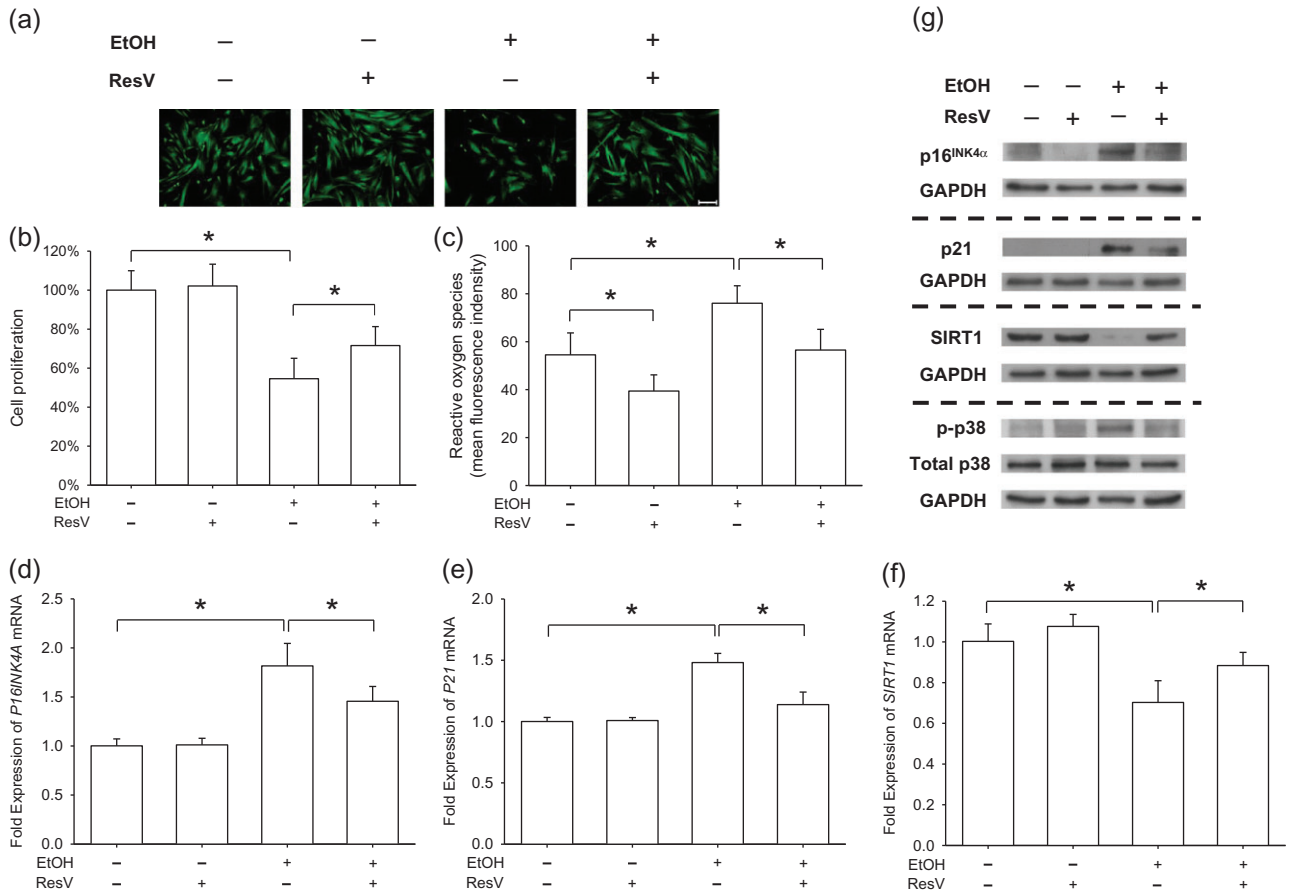

Fig. 4. ResV prevented EtOH-induced premature senescence by activation of SIRT1. BM-MSCs were treated with 10 μM ResV to activate SIRT1 in the presence of 250 mM EtOH. (**a**) Representative images labeled by FDA showed cell density and morphology. Scale bar = 200 μm. (**b**) Cell proliferation was determined by the CCK-8 assay. Absorbance was determined at 450 nm and was normalized to the level of untreated cells. (**c**) Measurement of intracellular ROS in EtOH-treated and ResV-treated BM-MSCs. (**d–f**) Real-time RT-PCR was used to measure the mRNA levels of *P16INK4A* (**d**), *P21* (**e**) and *SIRT1* (**f**). (**g**) Protein levels of $p16^{INK4\alpha}$, p21 and SIRT1 and phosphorylated levels of p38 were analyzed by western blot assays. Values are the mean ± SD of eight independent experiments ($n = 8$) in CCK-8 assays, four independent experiments ($n = 4$) in ROS assays, and four independent experiments ($n = 4$) in real-time RT-PCR experiments. Statistically significant differences are indicated by $^*P < 0.05$.

rescuing cell proliferation (Borodkina *et al.*, 2014). However, Umoh *et al.* showed that acute treatment with low-dose EtOH (5 mM) decreased the gene expression of p38 in cardiocytes (Umoh *et al.*, 2014). We speculate that the opposite effects of EtOH on p38 activation were due to the concentrations and exposure time of EtOH treatments. More importantly, we found that EtOH-induced premature senescence in BM-MSCs was accompanied by a down-regulation of SIRT1. More notably, during 250 mM EtOH treatment, the protein levels of SIRT1 in BM-MSCs declined more dramatically than its mRNA levels. In hepatocytes, EtOH treatments impaired cytosolic protein folding, evoked the unfolded protein response, and induced endoplasmic reticulum stress (Howarth *et al.*, 2012). Therefore, the exposure of BM-MSCs to EtOH at high concentrations affected not only the transcription stage but also post-translational modifications and protein degradation. However, the supplementation with ResV, a SIRT1 activator, was sufficient to suppress senescence phenotypes, including enhanced proliferation, attenuated ROS and suppressed levels of senescence-associated transcriptional factors, suggesting that activation of SIRT1 by ResV seems to be a new strategy for preventing oxidative stress- or EtOH-induced senescence in MSCs.

The impaired osteogenic potential of BM-MSCs has been considered a major cause for alcohol-induced osteoporosis (Gong and Wezeman, 2004). When exposing to 250 mM EtOH, matrix mineralization by BM-MSCs was dramatically repressed compared to untreated cells. However, only a slight decrease was observed in the gene expression of osteoblast-specific markers. We speculated that this discrepancy was caused by the different impact EtOH has on different stages of osteogenic differentiation of BM-MSCs. Treatments with high doses of EtOH hindered BM-MSCs from the mineralization stage, but did not completely inhibit the expression of osteoblast-specific genes, such as *COL1A1* and *RUNX2*, suggesting that EtOH treatments had stronger inhibitory effects on the late rather than the early stage of osteogenic differentiation. Although ResV treatment did not completely recover the proliferative capacity of EtOH-treated cells, the proliferation was partially rescued. More importantly, treating BM-MSCs with ResV restored the inhibited osteogenic differentiation. The underlying mechanisms by which ResV improved EtOH-inhibited osteogenic differentiation possibly involved peroxisome proliferator-activated receptor γ (PPARγ). Targeting PPARγ by siRNA was effective in repressing alcohol-induced adipogenic differentiation of BM-MSCs (Huang *et al.*, 2010).

CONCLUSION

The data from this investigation demonstrate that EtOH induces premature senescence in BM-MSCs in a dose-dependent manner. The

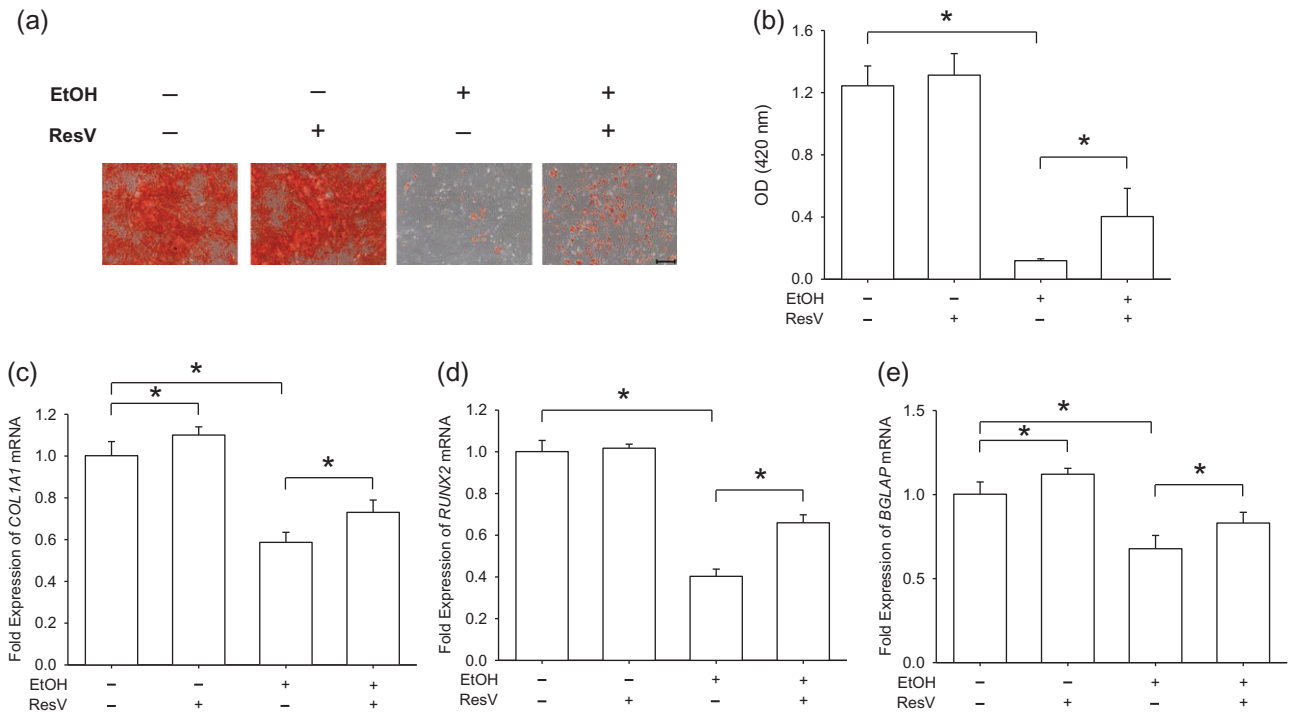

Fig. 5. ResV rescued EtOH-inhibited osteogenic differentiation of BM-MSCs. (**a**) Representative images of mineralized extracellular matrix stained by Alizarin Red S. Scale bar = 200 μm. (**b**) Quantification of matrix mineralization. The stained mineral layers were treated with perchloric acid and absorbance was measured at 420 nm. (**c**–**e**) The mRNA levels of osteoblast-specific marker genes, including *COL1A1* (**c**), *RUNX2* (**d**) and *BGLAP* (**e**) were measured by real-time RT-PCR. Values are the mean ± SD of four independent experiments ($n = 4$) in Alizarin Red S staining and real-time RT-PCR experiments. Statistically significant differences are indicated by $^*P < 0.05$.

underlying mechanisms involved excessive accumulation of intracellular ROS and down-regulation of SIRT1. EtOH-mediated premature senescence was responsible for impaired osteogenic differentiation of BM-MSCs. Activation of SIRT1 by ResV was effective in ameliorating EtOH-induced senescence phenotypes by recovering cell proliferation and rescuing impaired osteogenesis. Based on these findings, we suggest that prevention of premature senescence in BM-MSCs through activating SIRT1 could be a novel strategy for the protection of alcohol-induced BM-MSC dysfunction and osteoporosis.

ACKNOWLEDGEMENT

The authors are grateful to Suzanne Danley (West Virginia University, USA), Catherine Dyck (University of Waterloo, Canada) and Paula Sahyoun (University of Waterloo, Canada) for carefully reviewing and editing the manuscript. This work was supported by the National Natural Science Foundation of China (No.31570978, No.21574091); the Natural Science Foundation of Jiangsu Province (No.BK20140323); the National Institutes of Health (NIH) (AR062763-01A1 and AR067747-01A1) and an Established Investigator Grant from Musculoskeletal Transplant Foundation (MTF) to M.P.; and the Priority Academic Program Development of Jiangsu Higher Education Institutions (PAPD).

CONFLICTS OF INTEREST STATEMENT

None declared.

REFERENCES

Aldahmash A. (2015) Skeletal stem cells and their contribution to skeletal fragility: senescence and rejuvenation. *Biogerontology* **17**:297–304.

Bonyadi M, Waldman SD, Liu D, *et al.* (2003) Mesenchymal progenitor self-renewal deficiency leads to age-dependent osteoporosis in Sca-1/Ly-6A null mice. *Proc Natl Acad Sci U S A* **100**:5840–5.

Borodkina A, Shatrova A, Abushik P, *et al.* (2014) Interaction between ROS dependent DNA damage, mitochondria and p38 MAPK underlies senescence of human adult stem cells. *Aging* **6**:481–95.

Chen JR, Lazarenko OP, Haley RL, *et al.* (2009) Ethanol impairs estrogen receptor signaling resulting in accelerated activation of senescence pathways, whereas estradiol attenuates the effects of ethanol in osteoblasts. *J Bone Miner Res* **24**:221–30.

Chen X, He F, Zhong DY, *et al.* (2015) Acoustic-frequency vibratory stimulation regulates the balance between osteogenesis and adipogenesis of human bone marrow-derived mesenchymal stem cells. *Biomed Res Int* **2015**:540731.

Fusco S, Maulucci G, Pani G. (2012) Sirt1: def-eating senescence? *Cell Cycle* **11**:4135–46.

Gong Z, Wezeman FH. (2004) Inhibitory effect of alcohol on osteogenic differentiation in human bone marrow-derived mesenchymal stem cells. *Alcohol Clin Exp Res* **28**:468–79.

Ho PJ, Yen ML, Tang BC, *et al.* (2013) H2O2 accumulation mediates differentiation capacity alteration, but not proliferative decline, in senescent human fetal mesenchymal stem cells. *Antioxid Redox Signal* **18**: 1895–905.

Howarth DL, Vacaru AM, Tsedensodnom O, *et al.* (2012) Alcohol disrupts endoplasmic reticulum function and protein secretion in hepatocytes. *Alcohol Clin Exp Res* **36**:14–23.

Huang Q, Zhang H, Pei FX, *et al.* (2010) Use of small interfering ribonucleic acids to inhibit the adipogenic effect of alcohol on human bone marrow-derived mesenchymal cells. *Int Orthop* **34**:1059–68.

Ko E, Lee KY, Hwang DS. (2012) Human umbilical cord blood-derived mesenchymal stem cells undergo cellular senescence in response to oxidative stress. *Stem Cells Dev* **21**:1877–86.

Krishnamurthy J, Torrice C, Ramsey MR, *et al.* (2004) Ink4a/Arf expression is a biomarker of aging. *J Clin Invest* **114**:1299–307.

Li J, Pei M. (2012) Cell senescence: a challenge in cartilage engineering and regeneration. *T*issue Eng Part B Rev **18**:270–87.

Maurel DB, Boisseau N, Benhamou CL, *et al*. (2012) Alcohol and bone: review of dose effects and mechanisms. *Osteoporos Int* **23**:1–16.

Nuttall ME, Gimble JM. (2000) Is there a therapeutic opportunity to either prevent or treat osteopenic disorders by inhibiting marrow adipogenesis? *Bone* **27**:177–84.

Pei M, Li J, McConda DB, *et al*. (2015) A comparison of tissue engineering based repair of calvarial defects using adipose stem cells from normal and osteoporotic rats. *Bone* **78**:1–10.

Pittenger MF, Mackay AM, Beck SC, *et al*. (1999) Multilineage potential of adult human mesenchymal stem cells. *Science* **284**:143–7.

Rachner TD, Khosla S, Hofbauer LC. (2011) Osteoporosis: now and the future. *Lancet* **377**:1276–87.

Romero AM, Palanca A, Ruiz-Soto M, *et al*. (2016) Chronic alcohol exposure decreases 53BP1 protein levels leading to a defective DNA repair in cultured primary cortical neurons. *Neurotox Res* **29**:69–79.

Tseng PC, Hou SM, Chen RJ, *et al*. (2011) Resveratrol promotes osteogenesis of human mesenchymal stem cells by upregulating RUNX2 gene expression via the SIRT1/FOXO3A axis. *J Bone Miner Res* **26**: 2552–63.

Umoh NA, Walker RK, Al-Rubaiee M, *et al*. (2014) Acute alcohol modulates cardiac function as PI3K/Akt regulates oxidative stress. *Alcohol Clin Exp Res* **38**:1847–64.

Vassallo PF, Simoncini S, Ligi I, *et al*. (2014) Accelerated senescence of cord blood endothelial progenitor cells in premature neonates is driven by SIRT1 decreased expression. *Blood* **123**:2116–26.

Vaziri H, Dessain SK, Ng Eaton E, *et al*. (2001) hSIR2(SIRT1) functions as an NAD-dependent p53 deacetylase. *Cell* **107**:149–59.

Vidal MA, Walker NJ, Napoli E, *et al*. (2012) Evaluation of senescence in mesenchymal stem cells isolated from equine bone marrow, adipose tissue, and umbilical cord tissue. *Stem Cells Dev* **21**:273–83.

Walsh JS, Eastell R. (2013) Osteoporosis in men. *Nat Rev Endocrinol* **9**: 637–45.

Wezeman FH, Gong Z. (2004) Adipogenic effect of alcohol on human bone marrow-derived mesenchymal stem cells. *Alcohol Clin Exp Res* **28**:1091–101.

Yahata T, Takanashi T, Muguruma Y, *et al*. (2011) Accumulation of oxidative DNA damage restricts the self-renewal capacity of human hematopoietic stem cells. *Blood* **118**:2941–50.

Zhou L, Chen X, Liu T, *et al*. (2015) Melatonin reverses H2O2-induced premature senescence in mesenchymal stem cells via the SIRT1-dependent pathway. *J Pineal Res* **59**:190–205.